100 lbs to Low Earth Orbit (LEO): Small-Payload Launch Options

Lead Author
P. Dimotakis

Contributors:
R. Garwin
J. Katz
J. Vesecky

October 1999

JSR-98-140

JASON
The MITRE Corporation
1820 Dolley Madison Boulevard
McLean, Virginia 22102-3481
(703) 883-6997

REPORT DOCUMENTATION PAGE

Form Approved
OMB No. 0704-0188

1. AGENCY USE ONLY (Leave blank)	2. REPORT DATE	3. REPORT TYPE AND DATES COVERED
	October 19, 1999	

4. TITLE AND SUBTITLE

100 lbs to Low Earth Orbit (LEO): Small-Payload Launch Options

5. FUNDING NUMBERS

13-988534-A4

6. AUTHOR(S)

P. Dimotakis, R. Garwin, J. Katz, J. Vesecky

7. PERFORMING ORGANIZATION NAME(S) AND ADDRESS(ES)

The MITRE Corporation
JASON Program Office
1820 Dolley Madison Blvd
McLean, Virginia 22102

8. PERFORMING ORGANIZATION REPORT NUMBER

JSR-98-140

9. SPONSORING/MONITORING AGENCY NAME(S) AND ADDRESS(ES)

Defense Advanced Research Projects Agency
3701 North Fairfax Drive
Arlington, Va. 22203-1714

10. SPONSORING/MONITORING AGENCY REPORT NUMBER

JSR-98-140

11. SUPPLEMENTARY NOTES

12a. DISTRIBUTION/AVAILABILITY STATEMENT

Approved for public release, distribution unlimited.

12b. DISTRIBUTION CODE

Distribution Statement A

13. ABSTRACT *(Maximum 200 words)*

In this report, we examine the options for launching small payloads to Low Earth Orbit (LEO). ``Small'' is taken as, approximately, m_p=100 lbm, or perhaps a small multiple of that. Various launch options are considered, including single- and multi-stage, ground- and air-launched rockets, as well as the potential advantages of an intermediate airbreathing boost stage. Fundamental constraints between payload-to-total mass ratio, in a variety of launch vehicles, reveal a simple scaling persisting to small payloads. As a consequence, similar \$/lbm-to-LEO-injection costs can be expected to apply to all launch vehicles developed for the purpose. Such small-payload, small-total-cost launch options should be regarded as a technology-enabling development that may well spawn new defense, as well as civilian options, and markets. We recommend that such launch options be examined in sufficient detail to determine practical objectives and development paths to bring low-cost, small-payload launch systems to the military and the market.

14. SUBJECT TERMS

15. NUMBER OF PAGES

16. PRICE CODE

17. SECURITY CLASSIFICATION OF REPORT	18. SECURITY CLASSIFICATION OF THIS PAGE	19. SECURITY CLASSIFICATION OF ABSTRACT	20. LIMITATION OF ABSTRACT
Unclassified	Unclassified	Unclassified	SAR

Contents

Abstract

In this report, we examine the options for launching small payloads to Low Earth Orbit (LEO). "Small" is taken as, approximately, $m_p = 100\,\text{lbm}$, or perhaps a small multiple of that. Various launch options are considered, including single- and multi-stage, ground- and air-launched rockets, as well as the potential advantages of an intermediate airbreathing boost stage. Fundamental constraints between payload-to-total mass ratio, in a variety of launch vehicles, reveal a simple scaling persisting to small payloads. As a consequence, similar \$/lbm-to-LEO-injection costs can be expected to apply to all launch vehicles developed for the purpose. Such small-payload, small-total-cost launch options should be regarded as a technology-enabling development that may well spawn new defense, as well as civilian options, and markets. We recommend that such launch options be examined in sufficient detail to determine practical objectives and development paths to bring low-cost, small-payload launch systems to the military and the market.

Preface and Acknowledgments

This study was conducted by the JASON group during the Summer Session of 1998, on behalf of DARPA. In addition to the references cited, we would like to acknowledge discussions and contributions made by,

- Tom Jackson, AFRL/PRSS, Wright-Patterson AFB, with inputs by,
  - Steven Mozes, AFRL, Wright-Patterson AFB; and,
  - Fred Billig, presently acting as consultant to AFRL, Wright-Patterson AFB;
- John Hicks, NASA Dryden FRL; and
- David Farless, JPL.

1 INTRODUCTION AND CHARGE

In this report, we examine the possibility of whether small Low-Earth-Orbit (LEO) payloads, specifically, payloads with mass,

$$m_{\rm p} \simeq 100\,{\rm lbm} \simeq 50\,{\rm kg}, \qquad \text{(1-1a)}$$

indicate alternative launch/delivery options, different from ones available today.

Modern spacecraft technology, and especially sensors and electronics, can reduce the payload mass needed to accomplish space missions, such as communications, Earth remote sensing, exploration of the Earth's space environment, refueling/resupply of larger LEO satellites, etc. High launch costs (ca. $20\,{\rm k\$/lbm}$)[1] for small satellites/payloads ($100\,{\rm lbm} \lesssim m_{\rm p} \lesssim 100\,{\rm kg}$), however, have hampered implementation of new technology and, hence, cost reduction in space missions, by limiting the number of small satellite experiments. It is easily argued that lowering the cost threshold for getting small payloads into space will more than compensate for the research and development costs involved, by increasing the overall cost-effectiveness of using space for science, military, as well as commercial applications. Tethered satellites, new sensors, station-keeping of multiple satellites, deployable antennas, as well as innovations in propulsion, structure, power and thermal control, are examples of areas where small satellites can play important roles in advancing spacecraft technology and technique that would increase their effectiveness and lower costs.

For the purposes of this study, the possibility of total payloads, $m_{\rm tot}$, that are a small multiple of $m_{\rm p}$ is also considered, *i.e.*,

$$m_{\rm tot} = N\,m_{\rm p} \qquad \text{where} \qquad N = 1, 2, 3, \ldots\ , \qquad \text{(1-1b)}$$

but not so large that presently-available launch options may be considered adequate. By way of reference, and as will be discussed below, the nearest,

[1] Here, 'lbm' refers to pounds-mass of payload.

presently-available options correspond to,

$$N \approx \begin{cases} 6\,, & \text{for the } \textit{Pegasus}\text{, with estimated launch costs: 20-25 \$k/lbm;} \\ 40\,, & \text{for the } \textit{K-1}\text{, with projected launch costs: 1.5-2.5 \$k/lbm,} \end{cases} \tag{1-1c}$$

where *Pegasus* is the air-launched 3-stage solid-fueled rocket capability developed by Orbital Sciences Corp., and *K-1* is the low-cost, ground-launched liquid-fueled rocket presently under development by Kistler Aerospace Corp. The latter is expected to be operational within the next two years, or so. Actual numbers will depend on LEO altitude and inclination, with specific LEO-injection costs (\$k/lbm) for the *K-1* yet to be demonstrated, as will also be discussed below.

2 INSERTION TO LEO

A satellite in a circular orbit requires a speed, $U_{\rm co}$, given by the balance between the centripetal and gravitational accelerations. This balance requirement yields,

$$U_{\rm co} \simeq \frac{7.9\,{\rm km/s}}{(1 + h/R_{\rm E})^{1/2}} , \tag{2-1a}$$

where, h is the Circular Orbit Altitude (COA) and

$$R_{\rm E} \simeq 6.3 \times 10^3\,{\rm km} , \tag{2-1b}$$

is the Earth's radius.

At a typical speed of $U_{\rm co} \simeq 7.7\,{\rm km/s}$, as required for LEO insertion, and a payload mass, $m_{\rm p}$, such a satellite will have acquired a specific kinetic-energy increment of,

$$\frac{\Delta{\rm KE}}{m_{\rm p}} \simeq \frac{1}{2} U_{\rm co}^2 \simeq 30\,{\rm MJ/kg} . \tag{2-2a}$$

For a circular-orbit altitude of, say, $h \simeq 600\,{\rm km}$, a specific potential-energy increment of,

$$\frac{\Delta{\rm PE}}{m_{\rm p}} \simeq g\,h \simeq 6\,{\rm MJ/kg} , \tag{2-2b}$$

is also required. This brings the total required specific-energy increment to,

$$\frac{\Delta{\rm E}}{m_{\rm p}} = \frac{\Delta{\rm KE} + \Delta{\rm PE}}{m_{\rm p}} \simeq 36\,{\rm MJ/kg} . \tag{2-2c}$$

Interestingly, we have,

$$\Delta{\rm PE} \approx \frac{1}{5} \Delta{\rm KE} , \tag{2-2d}$$

i.e., most of the required energy increment is kinetic.[2]

[2]Since 1 kWhr = 3.6 MJ, the total specific-energy cost would be less than \$1/lbm, at, say, 20*c*/kWhr. Needless to say, it takes *mechanism* and *thrust* to inject a payload to LEO, not (just) *energy*.

Low-Earth Orbit altitude is typically determined by a target orbit lifetime, t_{orbit}, which is a function of the (mean) drag experienced by the satellite, which progressively decreases the (kinetic) energy and altitude. While this is a complex function of many variables, orbit lifetime is primarily dictated by,

- the (initial) orbit altitude, h;
- the so-called (dimensional) ballistic coefficient,

$$\beta \equiv \frac{m_{\text{p}}}{C_{\text{D}} A} , \tag{2-2e}$$

  typically expressed in units of kg/m^2, and
- launch phasing with respect to the solar cycle.

The latter in view of the dependence of the behavior of high-altitude (above 150 km) atmospheric temperature and, therefore, density on solar min/max activity. In this environment (rarefied-gas flow), the drag coefficient, as it appears in the ballistic coefficient, is in the range of $C_{\text{D}} \approx 2 - 4$, with A the cross-sectional area perpendicular to the flight path (*cf.* Eq. 2-2e).

Sample ballistic coefficients are summarized in Figure 1, which plots data compiled in Larson & Wertz (1992, Table 8–3). As can be appreciated, this quantity does not lend itself to any obvious scaling with size (read, m_{p}), depending (strongly) on whether the spacecraft employs solar panels, for example, and, if so, on their relative orientation to the orbit trajectory, which is, typically, not under control since they must be oriented to face the sun.

The results of sample simulations of orbit lifetimes for three representative ballistic coefficients are depicted in Figure 2 (Larson & Wertz 1992). As expected, orbit lifetime is a strong function of LEO altitude, h. We note that since the LEO payload-delivery capability (m_{p}) of a given launcher depends on the initial orbit altitude and inclination, there are potentially-important tradeoffs between payload and expected lifetime-in-orbit that can be exploited to advantage for small, low-cost spacecraft. The

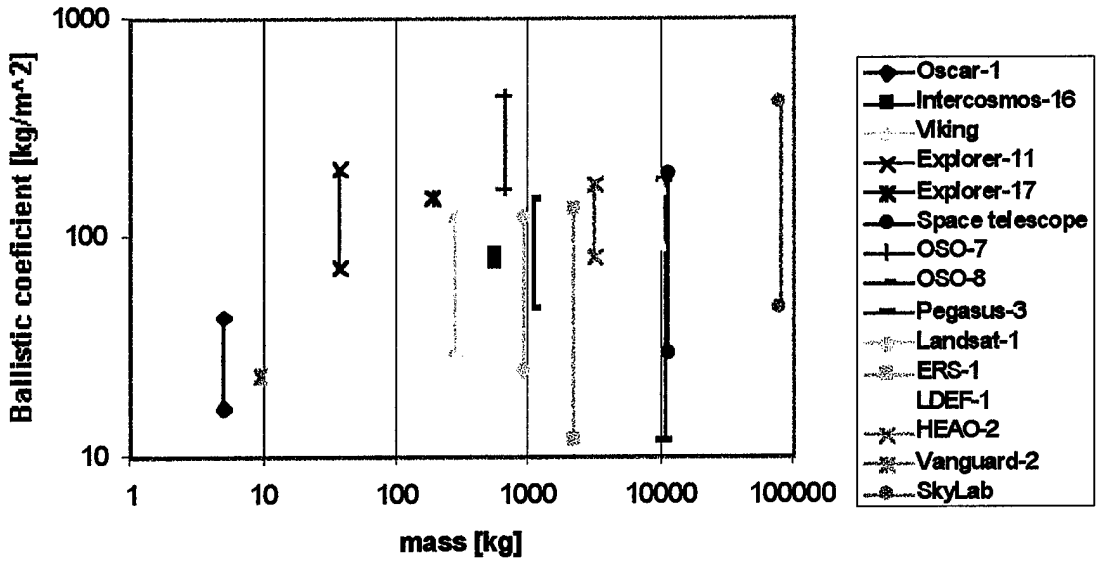

Figure 1: Range of ballistic coefficients (*cf.* Eq. 2-2e) for sample spacecraft (data from Larson & Wertz 1992, Table 8–3). Values depend on orientation (see text).

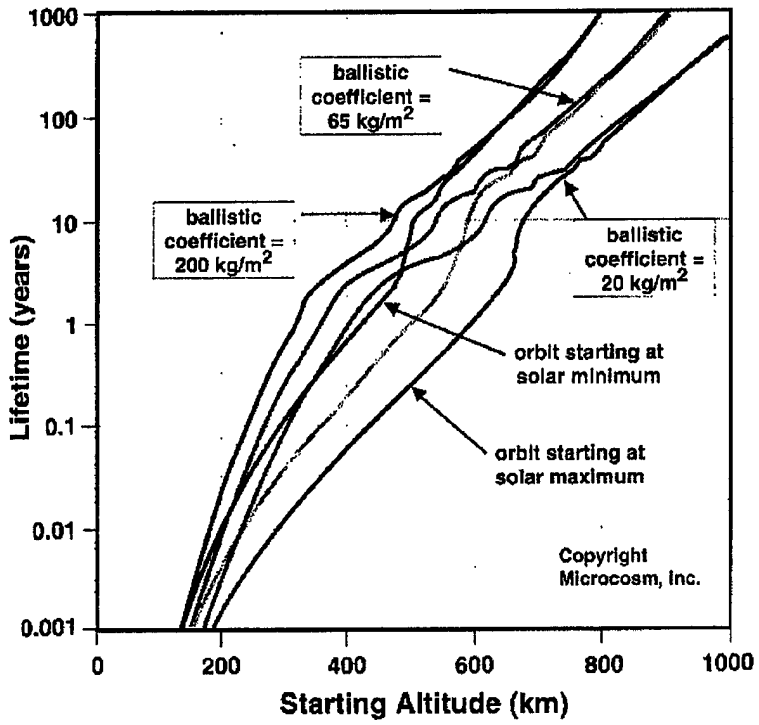

Figure 2: Satellite lifetimes as a function of initial orbit altitude, for representative ballistic coefficients (Larson & Wertz 1992, Fig. 8–13).

latter might adequately serve their purpose with an expected orbit lifetime of, say, $1 - 2$ months; an option not typically exercised intentionally for larger/more-expensive satellites.

3 LEO PAYLOAD

The final mass, $m_{\rm f}$, delivered to Low-Earth Orbit scales with the Gross Take-Off Weight (GTOW) of the launcher, being a function of the rocket-fuel characteristics. This is typically comprised of the mass of the payload, $m_{\rm p}$, and the balance of the mass of any structural rocket components, $m_{\rm s}$ ("parasitic" mass), delivered along with the payload, *i.e.*,

$$m_{\rm f} \;=\; m_{\rm p} + m_{\rm s} \;. \tag{3-1}$$

The essential elements of the payload-to-GTOW mass scaling can be understood in terms of a momentum control-volume analysis in the ascending rocket frame. In particular, we have,

$$\frac{d}{dt}\int_V \mathbf{u}\, m + \int_A \mathbf{u}\,\dot{m} \;=\; \underbrace{-\int_A p\,\mathbf{S}}_{\rm external-pressure} \quad \underbrace{+\int_A \tau\cdot\mathbf{S}}_{\rm skin-friction} + \int_V (\mathbf{g}-\mathbf{a}_{\rm rel})\,\mathbf{m}\;, \tag{3-2}$$

where V is the (rocket-frame) control volume, A its bounding surface (rocket exterior), $\mathbf{u}$ the velocity of differential mass elements in the rocket (control-volume) frame, $\dot{m}$ the differential mass flux through the control volume (rocket exhaust), $\mathbf{g}$ the acceleration of gravity, and $\mathbf{a}_{\rm rel}$ the acceleration of the rocket (control-volume) frame relative to the (common $\mathbf{F}$ and $\mathbf{g}$) reference frame. The differential mass-rate element, $\dot{m}$, in the area integral on the left-hand side is taken to be positive for outgoing mass crossing the control volume.

Performing the integrations and taking the component along the direction of motion, we then have,

$$\frac{\rm d}{\rm dt}\,(m\,u) \;-\; u_{\rm e}\,\dot{m}_{\rm e} \;=\; F_p \;+\; F_\tau \;-\; m\,\left(g\,\sin\theta + \ddot{X}\right)\;, \tag{3-3a}$$

where, $m = m(t)$ is the decreasing rocket mass, here, u is the (typically negligible) velocity of the rocket center of mass in the rocket (control-volume) frame, $u_{\rm e}$ is the rocket-exhaust velocity (here assumed to be perfectly aligned,

opposite the direction of travel),

$$\dot{m}_{\rm e} = -\frac{{\rm d}m}{{\rm d}t} \ , \tag{3-3b}$$

is the mass rate of the rocket exhaust,

$$F_p = -\int_A p\,\mathbf{S}\cdot\hat{\mathbf{U}} \tag{3-3c}$$

and

$$F_\tau = \int_A \tau\cdot\mathbf{S}\cdot\hat{\mathbf{U}} \ , \tag{3-3d}$$

are the components of the surface-pressure (includes form drag) and skin-friction (drag) contribution in the flight direction, $\hat{U} = \mathbf{U}/U$, respectively, θ is the angle subtended between the rocket travel velocity vector, $\mathbf{U}$, and the horizontal, and $X = U/t$ is the rocket-frame (control-volume) coordinate origin in the force-reference (*e.g.*, launch) frame.[3]

Assuming a constant rocket exhaust velocity, *i.e.*, if $u_{\rm e}$ and $\dot{m}_{\rm e}$ are assumed (approximately) constant (typically, largely as dictated by the combustion characteristics of the rocket propellants), we can write,

$$m\left(\dot{u}+\ddot{X}\right) = F_p + F_\tau + \dot{m}_{\rm e}\,(u_{\rm e}+u) - m\,g\,\sin\theta \ ,$$

and, to an excellent approximation (since $\dot{u} \ll \ddot{X} = \dot{U}$ and $u \ll u_{\rm e}$),

$$m\,\dot{U} \simeq \dot{m}_{\rm e}\,u_{\rm e} + F_p + F_\tau - m\,g\,\sin\theta \ , \tag{3-4}$$

where $U = \dot{X}$ is the rocket speed in our (say, Earth) reference frame. For a rocket, initially vertically ($\sin\theta = 1$) at rest ($U = 0$) on the ground, $F_p = F_\tau = 0$. We must evidently have $\dot{m}_{\rm e}\,u_{\rm e} > -m\,g$ for lift-off.

It is useful to partition the F_p and F_τ (surface-integral) contributions to the surface integral of the pressure over the rocket-exhaust area, $A_{\rm e}$, and the rest of the rocket exterior surface. This allows us to write,

$$F_p + F_\tau \simeq (p_{\rm e} - p_\infty)\,A_{\rm e} - D \ , \tag{3-5}$$

[3]The rocket community sometimes writes this relation as the familiar $F = m\,a = m\,u/t$, the so-called, "Newton's Law" (the quotes because he never said such a thing), instead of $F = P/t = (mu)/t$, which is what Sir Isaac argued for. The discrepancy is then corrected by including a $u(-m/t) = u_{\rm e}\,\dot{m}_{\rm e}$ term as a separate thrust term on the other side.

where p_e is the area-averaged pressure over the rocket-exhaust area, p_∞ is the ambient pressure some distance away from the rocket, and D is the drag. For a supersonic exhaust, p_e will be higher, or lower, than p_∞, depending on whether the rocket nozzle discharges as an underexpanded or overexpanded jet, respectively. At the higher altitudes, where most of the kinetic energy will be acquired, $p_\infty \to 0$, the supersonic jet will be underexpanded, and this term may not be negligible, depending on the rocket nozzle design.

It is useful to scale the drag, D, with $\rho U^2/2$, expressing it in terms of a drag coefficient, C_D, *i.e.*,

$$D = \frac{1}{2} C_D \rho U^2 A \tag{3-6a}$$

with ρ the (local) density of the air (which decreases with altitude), A the total cross-sectional area of the rocket normal to the direction of travel, and

$$C_D \simeq C_D(Ma, \alpha; \text{ rocket shape}) \ , \tag{3-6b}$$

with Ma the Mach number and α is the angle of attack. At $\alpha \approx 0$, a useful estimate for a typical rocket for the portion of the trajectory in the atmosphere is $0.05 \lesssim C_D \lesssim 0.15$, except around $Ma \approx 1$, where it will peak, reaching values in the range, $C_D \approx 0.15 - 0.3$, or so.[4] Combining, we then have,

$$m\dot{U} \simeq \mathcal{T} - D - W \sin\theta \ , \tag{3-7a}$$

where,

$$\mathcal{T} = \dot{m}_e u_{eq} \ , \tag{3-7b}$$

is the thrust (for a chemical rocket), with

$$u_{eq} = u_e + \frac{(p_e - p_\infty) A_e}{\dot{m}_e} \ , \tag{3-7c}$$

[4]Actual values will depend on rocket shape, with lower values for aerodynamic/slender rockets and higher values for more bluff shapes. Values quoted here are (much) smaller than the ones that correspond to the ballistic coefficients for spacecraft. The latter operate in rarefied-gas flow (mean-free path not small compared to body dimensions) with much-higher attendant C_D's.

the *equivalent* (or, effective) *exhaust velocity* (*e.g.*, Hill & Peterson 1992), D is the drag (Eq. 3-6a), and $W = m(t)\, g$ is the rocket weight at time t.

There is no difficulty integrating Eq. 3-7a, substituting empirically-known, or measured, expressions for $C_{\rm D}$, as a function of velocity (actually, as a function of the Reynolds and Mach numbers). We note that early on, however, gravity (weight) will be dominant with drag negligible, by comparison. Subsequently, as the rocket mass,

$$m(t) \;=\; m_0 \,-\, \int_0^t \dot{m}_{\rm e}\, t \;\simeq\; m_0 \,-\, \dot{m}_{\rm e}\, t \;, \tag{3-8}$$

decreases with continuing fuel expenditure — m_0 is the initial rocket mass or, "gross-take-off 'weight'" (GTOW), drag will become relatively more important.

Finally, the rocket will be moving in a rarefied environment ($\rho, p_\infty \rightarrow 0$), with $p_\infty A_{\rm e}, D, mg\sin\theta \ll \dot{m}_{\rm e} u_{\rm eq}$, and we'll have the approximate balance,

$$m\dot{U} \;\simeq\; \dot{m}_{\rm e}\, u_{\rm eq} \;\simeq\; (\, m_0 \,-\, \dot{m}_{\rm e}\, t\,)\, \dot{U} \;, \tag{3-9}$$

which describes a "horizontal" rocket in space. Integrating,

$$\frac{U}{u_{\rm eq}} \;=\; \frac{\dot{m}_{\rm e}\, t}{m_0 \,-\, \dot{m}_{\rm e}\, t} \;,$$

we have for the final mass, $m_{\rm f}$, delivered at a final speed, $U_{\rm f}$, or *mass ratio* (Sutton & Ross 1976), of

$$MR \;\equiv\; \frac{m_{\rm f}}{m_0}; \simeq\; e^{-U_{\rm f}/u_{\rm eq}} \;, \tag{3-10}$$

where $u_{\rm eq}$ is the equivalent exhaust velocity (Eq. 3-7c), above.

The ratio of the final to the initial mass, in other words, is (approximately) a function of the final velocity (increment) and the (equivalent) exhaust velocity, only. Equation 3-10, or its differential counterpart (Eq. 3-9), are sometimes referred to as the *rocket equation*. The orbit-delivery scaling described by Eq. 3-10 can be substantially improved by *staging* the rocket, which allows parasitic mass to be discarded during the orbit-injection process. The preceding analysis can be amended in a straightforward manner

to accommodate such rocket staging in the description, by summing successive applications over the number of stages, *e.g.*, Hill & Peterson (1992, pp. 481–490), Fortescue & Stark (1995, pp. 188–191).

As can be appreciated from these results, for a given total fuel mass expenditure, there is a great premium in operating the rocket with as high an exhaust velocity, u_e, as is feasible. For a chemical rocket, this is a function of the fuel reactants and the ensuing combustion. In particular, since the maximum exhaust velocity from a pressurized plenum (rocket combustion chamber) into a given back pressure is a function of the temperature (stagnation enthalpy) in the plenum and, for a perfect gas, the ratio of specific heats, the exhaust velocity can be easily estimated. In particular, the higher the rocket propellant combustion temperature, the higher the exhaust velocity.

The total *impulse* imparted on the remaining rocket mass, at any one time, is given by (integrating Eq. 3-7a for $u_{eq} \simeq$ const.),

$$I = \int_0^t \mathcal{T}\, t \simeq m_{prop}\, u_{eq} \ , \tag{3-11a}$$

where $m_{prop} = m_{prop}(t)$ is the total mass of expelled propellants by time t. We may then write,

$$\frac{I}{m_{prop}} \simeq \frac{\mathcal{T}}{\dot{m}_e} = u_{eq} \ . \tag{3-11b}$$

Historically, u_{eq} is scaled by g, the acceleration of gravity on the earth's surface, to express the rocket-exhaust velocity in terms of the *specific impulse*, I_{sp}, *i.e.*,

$$I_{sp} \equiv \frac{u_e}{g} = \frac{\mathcal{T}/g}{\dot{m}_e} \ , \tag{3-12a}$$

typically expressed in seconds. For a chemical rocket, typical values are in the range (for sea-level pressure exhaust),

$$200\,\mathrm{s} \lesssim I_{sp} \lesssim 410\,\mathrm{s} \ , \tag{3-12b}$$

corresponding to exhaust velocities in the range,

$$2.0\,\mathrm{km/s} \lesssim u_e \lesssim 4.0\,\mathrm{km/s} \ , \tag{3-12c}$$

with the higher values corresponding to the daunting H_2/F_2 fuel/oxidizer pair, with a corresponding $I_{sp} \simeq 480\,s$ for exhaust to vacuum. Values for actual liquid propellants are listed in Table 1 (Fortescue & Stark 1996, Table 6.1), for exhaust to $p_\infty = 1\,bar$.[5]

We conclude by noting that the delivered payload-to-GTOW ratio,

$$\frac{m_p}{m_0} = \frac{m_p}{m_f} \times \frac{m_f}{m_0} , \tag{3-13}$$

will primarily be a function of:

a. the payload-to-parasitic mass of the (final) rocket stage,

b. the number of stages, and

c. the rocket-fuel specific impulse, I_{sp}.

While other parameters will also play a role, the ones listed above can be expected to dominate.

[5]There are benefits in I_{sp} as the exhaust pressure, p_∞, is lowered, especially if the rocket-nozzle exhaust area can be increased (added weight) accordingly. This is the reason why the (theoretical) I_{sp} to vacuum for the H_2/F_2 fuel/oxidizer pair differs from the value in Table 1.

Table 1: Liquid-propellant properties, calculated for a rocket combustion chamber stagnation pressure of $p_0 = 7\,\mathrm{MPa}$ (70 bar) and an ideal (isentropic) expansion to an exhaust pressure of $p_\infty = 0.1\,\mathrm{MPa}$ (1 bar). Data from Fortescue & Stark (1995, Table 6.1).

Fuel	Oxidizer * hypergolic	Molecular weight W products	Combustion temperature T_c [K]	Ideal specific impulse I_{sp} [s]	Mean density ρ [kg/m³]
H_2 (hydrogen)	O_2 (oxygen)	10.0	2980	390	280
	*F_2 (fluorine)	12.8	4117	410	460
Kerosene	O_2	23.4	3687	301	1020
	F_2	23.9	3917	320	1230
	RFNA (red fuming nitric acid)	25.7	3156	268	1355
	N_2O_4 (nitrogen tetroxide)	26.2	3460	276	1260
	H_2O_2 (hydrogen peroxide)	22.2	3008	278	1362
N_2H_4 (hydrazine)	O_2 (oxygen)	19.4	3410	313	1070
	*HNO_3 (nitric acid)	20.0	2967	278	1310
$(CH_3)_2NNH_2$ (UDMH -	O_2 (oxygen)	21.5	3623	310	970
unsymmetrical dimethyl hydrazine)	*HNO_3 (nitric acid)	23.7	3222	276	1220
Monopropellants					
N_2H_4		10.3	966	199	1011
H_2O_2		22.7	1267	165	1422

4 AVAILABLE LAUNCH VEHICLES

In assessing options for small-payload LEO insertion, it is useful to review available options. The two smaller-payload presently-, or near-term-available options mentioned earlier (Eq. 1-1a) are the *Pegasus* of Orbital Sciences Corporation, and the upcoming *K-1*, of Kistler Aerospace Corporation.

4.1 The Pegasus Launcher

The *Pegasus* is a three-stage, solid-rocket-motor (SRM), air-launched vehicle, released from a modified Lockheed L–1011 at an initial altitude of,

$$h_0 \simeq 38\,\text{kft} \simeq 12.3\,\text{km} \ , \tag{4-1a}$$

at a Mach number of $Ma_0 \simeq 0.8$, or an initial velocity of,

$$U_0 \simeq 0.25\,\text{km/s} \ , \tag{4-1b}$$

with an initial Gross-Take-Off-Weight (GTOW, *i.e.*, mass) of,

$$m_0 \simeq 50 \times 10^3\,\text{lbm} \simeq 27 \times 10^3\,\text{kg} \ . \tag{4-1c}$$

It is capable of delivering payloads to low-inclination, Circular Orbit Altitudes (COA) of,

$$m_\text{p} \simeq \begin{cases} 320\,\text{kg} & (700\,\text{lbm}), \quad \text{to 600 km COA}\,; \\ 270\,\text{kg} & (600\,\text{lbm}), \quad \text{to 800 km COA} \end{cases} \tag{4-1d}$$

(*cf.* Figure 3). Using the lower-COA payload figure, we see that the *Pegasus* payload mass ratio is given by,

$$\frac{m_\text{p}}{m_0} \simeq \frac{700}{50{,}000} \simeq 1.4\% \ . \tag{4-1e}$$

While this may appear small, such a payload mass ratio is actually on the high side. This is accomplished despite the SRM stages, which place the

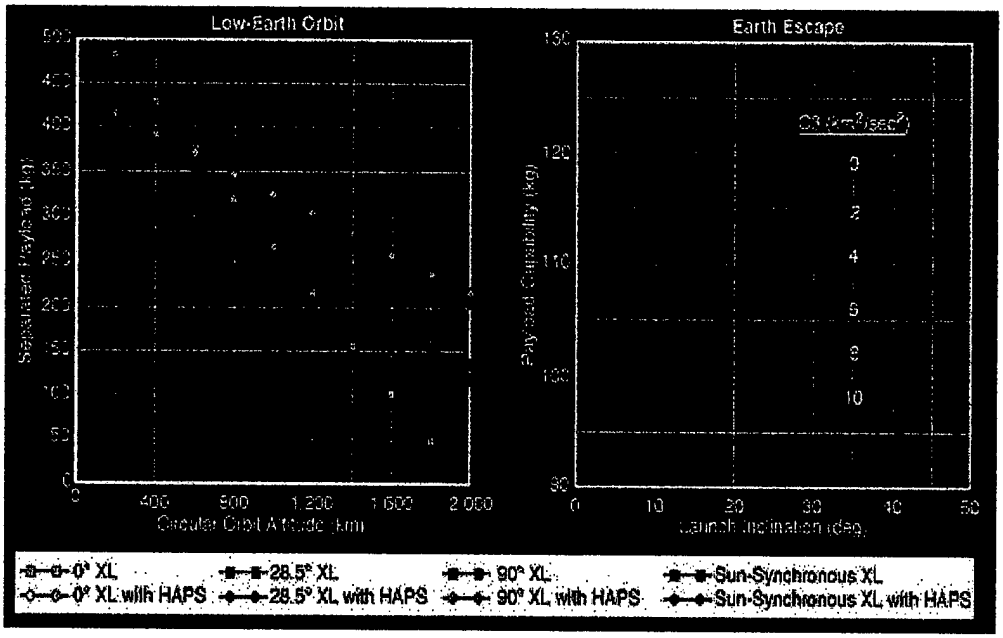

Figure 3: *Pegasus* payload performance figures (Orbital Sciences Corp. Web pages. Downloaded July 1998).

Pegasus on the lower half of the I_{sp} range (Eq. 3-12a). The main reason for this is the relatively-high-altitude air launch, which starts the launcher with some potential and kinetic energy, and, more importantly, with a lower drag (Eq. 3-6a), since (assuming a 10 km scale height),

$$\frac{\rho_{12.3\text{ km}}}{\rho_{\text{sea level}}} \approx e^{-12.3/10} \simeq 0.24 \qquad (4\text{-}2)$$

(recall linear density dependence of drag, Eq. 3-6a). A ground-launched rocket will have achieved sufficiently high speed by an altitude of $h \approx 12\,\text{km}$ that drag will be significant in the rocket-trajectory force balance (recall Eq. 3-7a).

At an estimated launch cost of \$15M,[6] specific payload launch costs for the *Pegasus* are, approximately,

$$(\$_{sp})_{\text{Pegasus}} \approx \$47{,}000/\text{kg} \ ,$$

with actual figures depending on what fraction of the vehicle payload capacity is utilized and orbit specifics (*cf.* Figure 3).

[6]Orbital Sciences Corp. Web pages. Downloaded July 1998.

4.2 The K–1 Launch Vehicle

The *K–1* launch vehicle, by Kistler Aerospace Corp., is a reusable, ground-launched, two-stage, kerosene/LOx propelled (higher I_{sp} than SRM's), launch vehicle, with a GTOW (mass) of,

$$m_0 \simeq 805{,}000\,\text{lbm} \simeq 366{,}000\,\text{kg} \ . \tag{4-3a}$$

It is capable of delivering a payload mass of,

$$m_p \simeq \begin{cases} 3200\,\text{kg} & (7000\,\text{lbm}), \quad \text{to } 600\,\text{km}/37°\text{COA}\,; \\ 1800\,\text{kg} & (4000\,\text{lbm}), \quad \text{to } 600\,\text{km}/90°\ \text{COA}\,. \end{cases} \tag{4-3b}$$

A plot of the payload-delivery capability as a function of orbit parameters is reproduced in Figure 4.

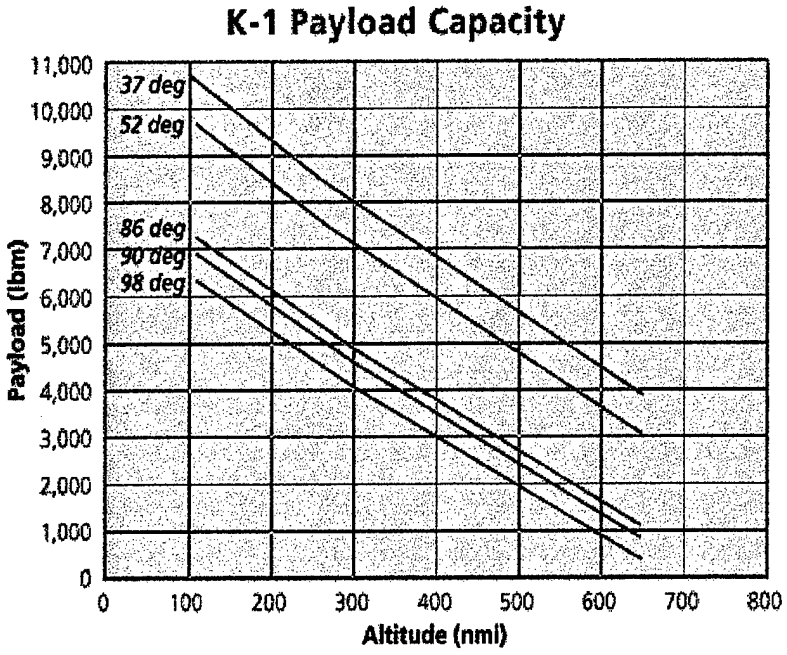

Figure 4: *K–1* payload performance figures (Kistler Aerospace Corp. Web pages, July 1998).

Accepting the lower-inclination orbit payload of 6000 lbm as a reference, we have a payload mass ratio for the *K–1* of,

$$\frac{m_{\rm p}}{m_0} \simeq \frac{6000}{805{,}000} \simeq 0.9\% \ , \qquad \text{(4-3c)}$$

i.e., roughly 2/3 that of the *Pegasus* launcher.

A test launch of the *K–1* is scheduled before the end of the 1998 calendar year. Kistler Aerospace (July 1998 Web pages) cites a $100M contract with Lockheed-Martin for 10 launches to take place in the next few years. *Aviation Week* (12 January 1998) estimates a cost of $17M per launch. Accepting the latter figure, we have a specific launch payload cost for the *K–1* of,

$$(\$_{\rm sp})_{\rm K-1} \approx \$5{,}300/{\rm kg} \ ,$$

or, roughly, 1/9 the specific payload cost for the *Pegasus*. Needless to say, the *K–1* has not flown yet and it would require launching a constellation of $N = 40$, $m_{\rm p} \simeq 50\,{\rm kg}$ satellites to achieve this specific cost.

4.3 Other Launchers

In assessing scaling with payload size, it is instructive to compare the statistics for the *Pegasus* and the *K–1* with those of other launch vehicles. These are summarized in Table 2 (data compiled from a variety of sources).

An important comparison to the *Pegasus* is the *Scout*, developed by NASA for small payloads starting in the late sixties and retired about 10 years ago. Its estimated launch price was referenced to 1998 $'s (*cf.* Table 2). It was a ground-launched, solid-propellant rocket, with a gross-take-off-weight (GTOW) very similar to the *Pegasus*. Its lower payload mass ratio,

$$\left(\frac{m_{\rm p}}{m_0}\right)_{\rm Scout} \simeq 0.9\% \ ,$$

can be attributed to the earlier technology involved but, primarily, the fact that it was a ground– *vs.* air-launch vehicle – drag is comparatively more

Table 2: Launcher statistics. GTOW denotes Gross Take-Off Weight (mass).

	GTOW/kg	Payload/kg	Launch-$M	Payload/GTOW	$/GTOW-kg	$k/Payload-kg	Notes
Scout	22,091	205	15	0.9%	679	73.3	a
Pegasus	22,727	318	15	1.4%	660	47.1	
Cosmos-3M	109,091	1,364	10	1.3%	92	7.3	
Titan-2	154,545	1,818	50	1.2%	324	27.5	
Atlas-1	164,591	2,259	65	1.4%	395	28.8	
Delta-2	232,273	2,273	50	1.0%	215	22.0	
Atlas-2A	187,727	1,536	87	0.8%	463	56.6	
Atlas-2AS	237,273	1,864	90	0.8%	379	48.3	
Delta-3	300,000	3,818	150	1.3%	500	39.3	
K-1	365,909	3,182	17	0.9%	46	5.3	b
Ariane-4	481,000	4,900	250	1.0%	520	51.0	
Proton-K	690,909	5,500	60	0.8%	87	10.9	
Ariane-5	740,000	6,900	300	0.9%	405	43.5	
X-33	1,360,000	13,636		1.0%			b
Titan-4	1,910,000	25,000	325	1.3%	170	13.0	
Space Shuttle	2,045,455	22,727	1,000	1.1%	489	44.0	

From: *Aerospace Source Book*, Aviation Week & Space Technology (12Jan98, 11Jan99)
A. R. Curtis (ed.), Space Almanac (2nd edition, Gulf Publishing, Houston, 1992)
Orbital Sciences Corp. Web pages (July 1998)
Kistler Aerospace Web pages (July 1998)
Ariane Web pages (July 1998)

Notes: a For reference (retired)
b Under development

important with decreasing vehicle size. The *Scout* addressed that issue by being very slender (high height-to-diameter aspect ratio). Nevertheless, the delivered payload mass ratio is comparable to the much larger $K - 1$.

The payload mass ratio, for all the launch vehicles in Table 2, is plotted in Figure 5. As can be seen, the data are clustered within a rather small range, *K–1*.

$$0.8\% \lesssim \frac{m_p}{m_0} \lesssim 1.5\% \ , \tag{4-4}$$

even as the gross take-off weight (GTOW) *ranges over roughly two orders of magnitude*, substantiating the validity of the approximations in the analysis in Section 3.[7]

It is also instructive to compare the specific payload costs for the launch vehicles in Table 2. These are plotted in Figure 6 as a function of the gross

[7]The nature of chemical bonds (enthalpies of formation of molecules) and molecular thermodynamics being what they are, it's worth noting that the earth would not have to be much larger for chemical propulsion (for the most part, all there is) to provide a near-inadequate means for escaping its pull.

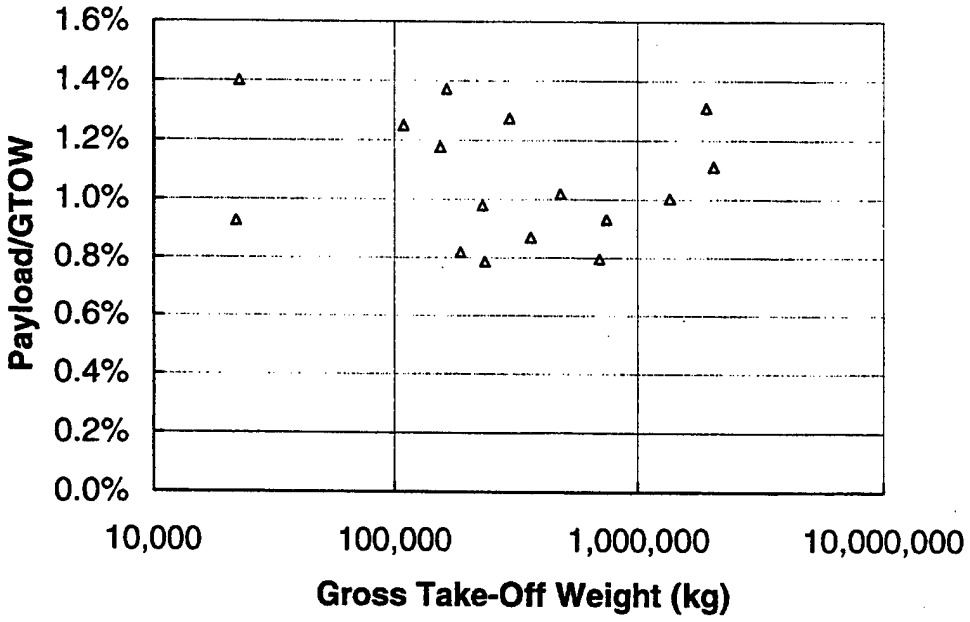

Figure 5: Payload-to-launch mass ratio for launchers listed in Table 2.

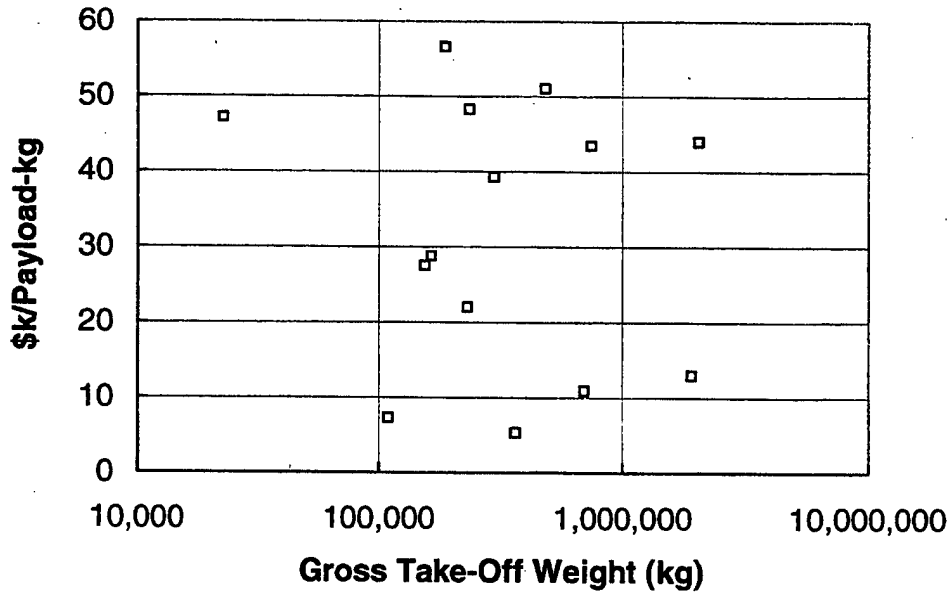

Figure 6: Estimated specific payload launch costs for launchers listed in Table 2. The two lower-cost options correspond to the Russian Cosmos-3M, for which actual costs are difficult to estimate, and the U.S. *K-1*, discussed above, the latter presently under development.

available and as less directly comparable to the rest. While these are clustered over a larger range (about a decade), *i.e.*,

$$5\,\text{k\$/kg} \lesssim \$_{\text{sp}} \lesssim 50\,\text{k\$/kg} \ , \tag{4-5}$$

we note no conspicuous correlation with gross-take-off weight (GTOW).[8]

In assessing these figures, we should note the general lack of pressure on the launch market imposed by the Space Shuttle. It is only recently that companies such as Kistler Aerospace (*K-1*) and a few others emerging at this time are capitalizing on the large margin between what can evidently be offered profitably as a specific launch cost to an expanding market and what has been available to date. A similar compilation one-to-two years from now may be expected to exhibit a clustering at the lower figures.

4.4 The X-33

We close this section by discussing the *X-33*, a half-scale demo version of *VentureStar*, a target commercial, single-stage-to-orbit (SSTO) vehicle, presently under development with Lockheed-Martin as the prime contractor. *VentureStar* has a January 2000 goal, based in part, on the outcome of *X-33* test flights that must demonstrate $Ma > 8$, within the continental U.S., *i.e.*, no orbital capability for the *X-33*.

VentureStar is designed as a ground-launched, fully-reusable, hydrogen/LOx-propellant, LEO-launch vehicle, with a gross take-off weight (launch mass) of,

$$m_0 \simeq 1{,}360{,}000\,\text{kg} \ , \tag{4-6a}$$

and a target payload to LEO of,

$$m_{\text{p}} \simeq 13{,}600\,\text{kg} \ , \tag{4-6b}$$

[8]By way of comparison, gold is valued at, roughly, 10 k\$/kg, at this time.

i.e., a target payload mass ratio of,

$$\left(\frac{m_{\rm p}}{m_0}\right)_{\rm X-33} = 1\% \ . \qquad \text{(4-6c)}$$

Its promise is low specific payload launch cost, with claims that it will be in the \$1,000/lbm range.[9]

At this writing, however, the *X-33* is having problems with its "Aerospike" engine, is slipping in schedule, its (parasitic) mass and drag are increasing, and may have a tough time making Mach 8.[10] There are also questions about the eventual *VentureStar* mass and whether it can close on the required SSTO velocity.

[9]NASA Administrator Dan Goldin (2 July 1996): "Our goal is a reusable launch vehicle that will cut the cost of a pound of payload to orbit from \$10,000 to \$1,000" (Lockheed Martin Web pages, X33, 23 July 1998 download).

[10]The New York Times (2 March 1999) reported the *X-33* as, " ... more than a year behind schedule for its first flight because of mounting technical problems." According to the report, the problems " ... affecting the *X-33* include difficulty in manufacturing its engines, a new design that has never flown before; trouble in making its lightweight, graphite-reinforced plastic fuel tanks, and excess weight that will reduce the craft's performance."

5 SMALL-PAYLOAD LAUNCH OPTIONS CONSIDERED

In evaluating technologies that should be considered, two options for a small-payload LEO-launcher were assessed:

1. a hybrid rocket that would include an airbreathing boost stage, and
2. a suitably-scaled, airlaunched, but otherwise conventional, rocket.

These will be discussed below.

5.1 A Hybrid Rocket with an Airbreathing Stage

It is easy to argue for the potential merits of a supersonic, airbreathing stage (SCRAMJET).[11] A very large fraction of the gross take-off weight of the Shuttle and the *X-33* is comprised of liquid oxygen (LOx), equal to 75% for the *X-33*, for example.

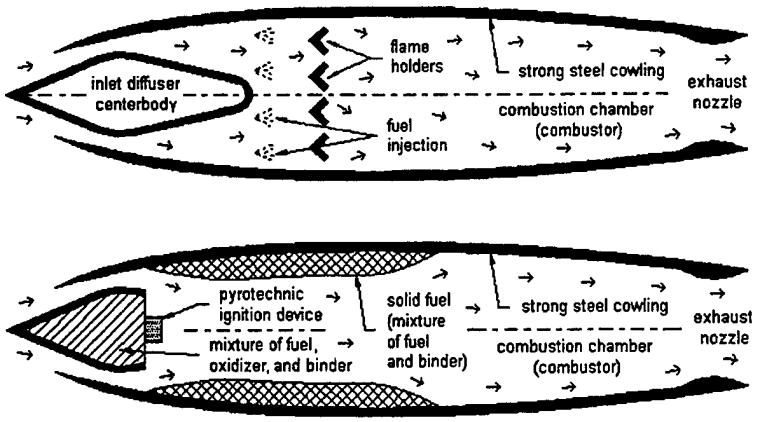

Figure 7: Liquid- (top) and solid-fueled ramjet schematics.

[11] "SCRAMJET" for Supersonic Combustion RAMJET.

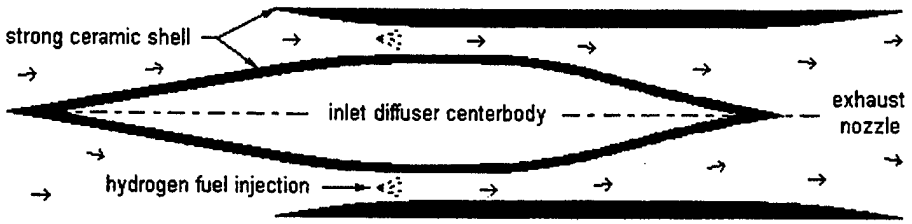

Figure 8: Scramjet schematic.

An airbreathing stage would utilize oxygen in the atmosphere, during the endoatmospheric portion of the ascent phase, and could potentially and qualitatively alter the inexorable payload (m_p) + parasitic (m_s) mass (Eq. 3-1) ratio scaling, leading (Eq. 3-10) to a payload mass ratio of $MR \approx 1\%$, or so, that conventional chemical rocketry delivers. This is illustrated by the potential corresponding values for the specific impulse, I_{sp}, which expresses the thrust, $\mathcal{T}$ (normalized by the gravitational acceleration, g), per unit mass exhaust rate, $\dot{m}_e$ (Eq. 3-12a). See also Heiser (1994).Heiser$_P DM$.94

In the case of a rocket, all the mass expelled as exhaust is mass originally carried, whereas, for an airbreather, only the fuel mass must be carried, with the oxidizer (air) mass contribution to the exhaust products ingested at the SCRAMJET aerodynamic inlet. This is illustrated in Figure 9, where the specific impulse for turbojets (*e.g.*, subsonic jets), ramjets (Figure 7),[12] and scramjets (Figure 8)[13] are compared to that of rockets.

Secondly, a vehicle with such an airbreathing stage could exploit the favorable lift-to-drag ratio of a suitably-designed body, ($L/D5$), even at high Mach numbers (*cf.* Figure 10) and gain some of the potential energy increment through lift. This, of course, would be subject to a variety of constraints. In particular, it must remain below an appropriate altitude during the airbreathing phase such that the oxygen number density remains high enough to sustain mixing-limited, sufficiently-rapid chemical kinetics to support completion of the combustion non-equilibrium radical species re-

[12]The SR-71 "Blackbird" is propelled by a combined-cycle turbojet/ramjet engine.
[13]Schematics from `http://www.millenial.org/~jwills/orbit/`.

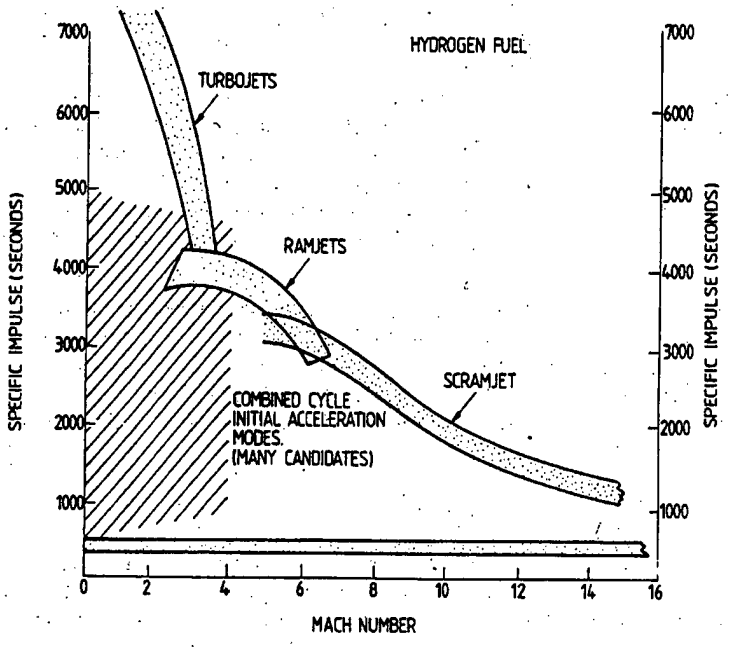

Figure 9: High-speed propulsion options in the earth's atmosphere. Specific impulse for chemical rockets is in the range $200\,\mathrm{s} \lesssim I_{\mathrm{sp}} \lesssim 400\,\mathrm{s}$ (bottom bar, *cf.* Table 1). From Fortescue & Stark (1995, Fig. 6.13).

combination steps. At the high internal-flow Mach numbers that must be considered, converting a sufficiently high fraction of the potentially available (chemical-formation) enthalpy conversion by the combustion process becomes increasingly difficult, as also required to overcome increasing internal losses.[14] Another way to view some of the issues is to appreciate that, as speed increases, the flow-residence/-mixing time, τ_{m}, through the combustor decreases, while the chemical-completion time, τ_χ, remains the same, or decreases with decreasing temperature/pressure. The Damköhler number, $Da \equiv \tau_{\mathrm{m}}/\tau_\chi$, then falls, decreasing the fraction of the chemical reactions that can be completed within the useful propulsor extent.

[14] As Mach number and $U^2/2$ increases, it becomes increasingly difficult to compensate for small fractional losses in $U^2/2$ in the internal flow by chemical (enthalpy) conversion through combustion, negating the potential propulsive benefits of the latter.

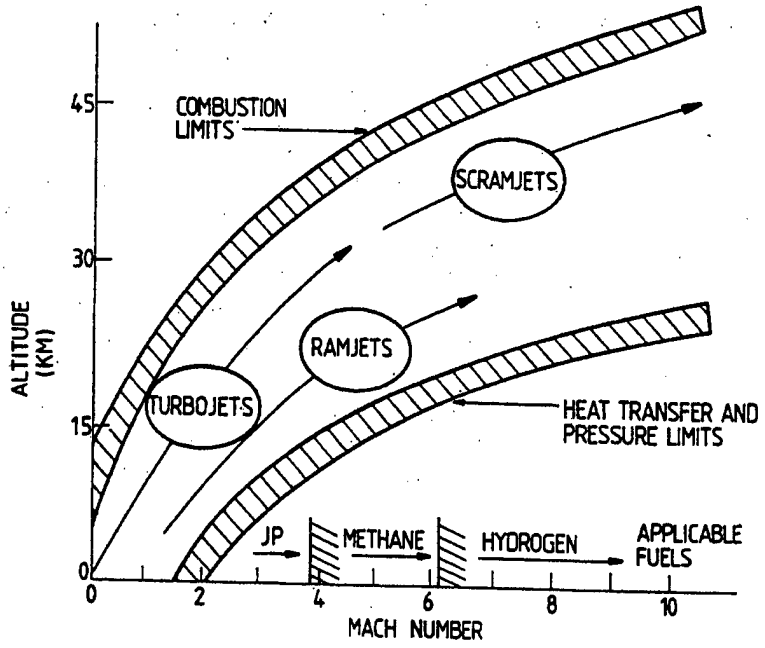

Figure 10: High-speed, airbreathing-propulsion trajectory constraints. (Fortescue & Stark 1995, Fig. 6.14).

An important advantage of Scramjet (Figure 8) propulsion is its potential simplicity. The complex air compression stages that comprise a large fraction of the weight and moving parts of a traditional gas turbine engine are obviated. Scramjet compression can be realized by an oblique shock wave, or a sequence of oblique shock waves (Figure 11), with (potentially) acceptably small attendant entropy production (total pressure losses).

To date, there has been a French flight demonstration of airbreathing thrust with a Ramrocket (Figure 12) on a Russian missile, to $Ma \simeq 5$,[15] The simplicity of such propulsion is evident, with an embedded solid rocket motor (SRM) booster for the initial propulsion phase that switches to solid-propellant, ramjet operation in a natural way.

A second test involved the NASA CIAM Scramjet and achieved full scram operating mode at Mach 6.5. It required a redesign of the Scramjet

[15]Craig Covault (February 1995), "French Flight Test Rocket-Ramjet Missile," Av. Week & Space Tech. **142**(9), 22.

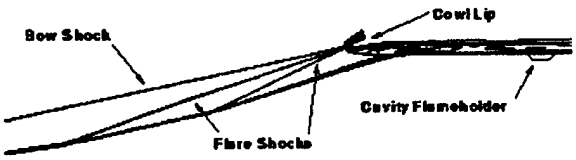

Figure 11: Ramjet inlet. Bow shock generated by nose point, to the left of the drawn schematic (*cf.* also 8 inlet). Further compression is realized by a succession of subsequent oblique shocks generated by small turning angles.

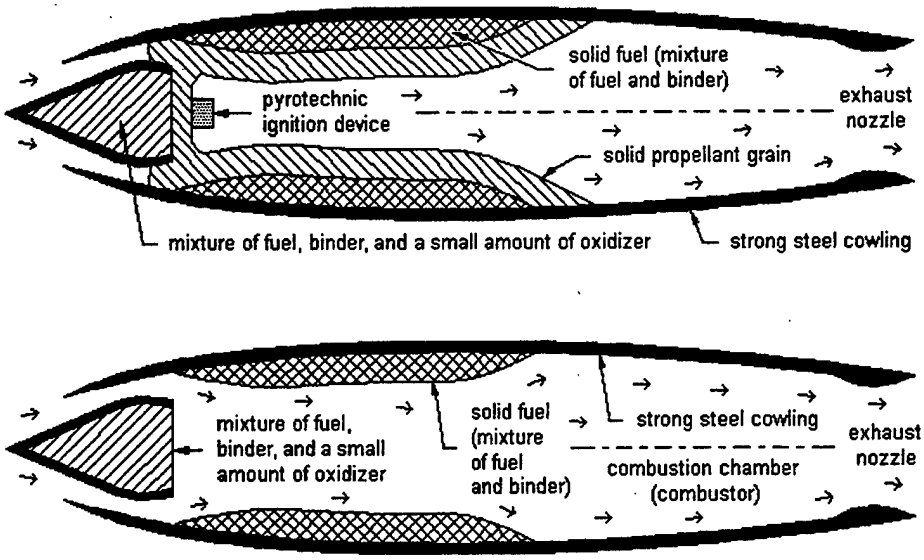

Figure 12: Ramrocket before launch (top) and shortly after launch (bottom).

combustor and active cooling system to handle the higher, sustained heat loads and a replacement of the inlet leading-edge material (Figure 11). The propulsor was carried on a Russian SA-5 rocket booster, modified to reduce weight by 124 kg and decrease drag by 6%. The flight launch took place in the Republic of Kazakhstan at the Sary Shagan test range some 300 mi north of the city of Alma Ata on the shores of Lake Balkash. The flight extended up to 170 km downrange to the west and lasted approximately 120 s. The initial 5 s boost was provided by four strap-on solid-rocket boosters. At 38 s into the flight, Scramjet engine operation and maximum cooling flow rate began as the rocket reached Mach 3.5. Between 56 s and 59 s into the flight, a new maximum Mach number of over 6.4 was achieved, at an altitude of about 22 km. Preliminary measurements and postflight analysis confirm that full supersonic combustion was achieved in the engine. Fueled engine operation continued for some 77 s until a commanded flight termination occurred 116 s into the flight. Based on preliminary postflight data analysis, supersonic combustion occurred through the length of the engine at approximately a stoichiometric fuel-air ratio. Positive thrust from the engine was also achieved as determined by the flight trajectory data. CIAM reports that this is the longest continuing operation ever achieved with their Scramjet in flight.[16] This test constitutes the first demonstration of Scramjet operation, to Mach 6.5.

A demonstration/development program that will explore air-breathing Scramjet propulsion is presently in progress. Dubbed the "Hyper-X", it will utilize a 30-inch long Scramjet engine fabricated by GASL, Inc. (Ronkonkoma, NY) as part of a research effort to demonstrate hypersonic propulsion technologies in flight. The Hyper-X vehicles, have been designated X-43 and will be boosted on the first stage of a modified Orbital Sciences Corp. *Pegasus* booster rocket and launched by NASA's B-52 from an altitude of 19 kft to 43 kft, depending on the mission. For each flight, the booster is slated to accelerate the X–43 to Mach 7 or 10 to altitudes up to 100 kft, where it will separate from the booster to demonstrate flight under its own power. A first test flight is scheduled in 2000 (Braukus al 1998).

[16]Excerpted from Aerospace America (June 1998), p. 28.

There is no question that airbreathing propulsion, with a final rocket-boost stage for orbit injection, holds the greatest promise of increasing the payload mass ratio beyond the range of figures discussed above. Even so, this propulsion can only serve as a stage of a total LEO-injection system. As we'll discuss below, only a portion of the kinetic energy, ΔKE (*cf.* Eq. 2-2a), can be attained by such an airbreathing stage. To achieve even that, an airbreather must remain within the atmosphere longer, gaining as much kinetic energy there as feasible. This dictates a thermal management system to contend with sustained aerodynamic heating at high Mach numbers, as contended with in the NASA/Russian CIAM test (above). Finally, fundamental associated science and technology issues are as yet unresolved. These include,

- the behavior of turbulence and expected efficacy of turbulent mixing in supersonic flow,
- ignition and flame-stability issues in non-premixed combustion at high strain rates,
- radical recombination within the propulsor extent,
- minimizing kinetic-energy losses in the internal flow,
- maintaining supersonic internal-flow in the presence of skin friction and heat addition (frictional/thermal choking),
- materials, thermal and endothermic-fuel management.

Unfortunately, research and development efforts to date have not adequately addressed these issues, despite the large national investment in the NASP (National AeroSPace plane) program.

Scramjet operation is inextricably intertwined with the fuel's chemical-kinetics and thermodynamics characteristics. Consider, first, a kerosene-type fuel, such as the standard military JP8. This has a high energy density (MJ/m^3), which implies a lower-cross-section vehicle and attendant supersonic-drag benefits. Thermal management at high Mach numbers is anticipated

through its use as an endothermic fuel, *i.e.*, by relying on thermal cracking in passages near the outer skin to produce lower molecular-mass species. This both removes the heat (enthalpy) of formation of these species from the body exterior and produces a more ignitable mixture.

Scramjet operation must wait for $Ma_{\min} \approx 4-5$, or so (*cf.* Figure 10). Such Mach numbers are necessary to maintain supersonic flow through the combustor, after (oblique-shock) compression (Eq. 11), and are also dictated by fuel-ignition and flame-stability considerations, where the high stagnation temperatures that increase quadratically with increasing Mach number are exploited. Attaining this initial Mach number would require a conventional initial rocket stage, however, or a Ramrocket stage (Figure 12).

An upper limit on Mach number of $Ma_{\max} \approx 8$ is anticipated by chemical-kinetics considerations as well as the capacity of JP8 fuel to remove aerodynamic heating endothermically. Referencing these Mach numbers to room-temperature air, as an approximation, we find that such a stage can, at most, attain a kinetic-energy increment fraction of the necessary total of,

$$\left(\frac{\Delta \mathrm{KE}}{\Delta \mathrm{KE}_{\mathrm{LEO}}}\right)_{4 \leq Ma \leq 8} \approx 9\% \ , \tag{5-7}$$

where $\Delta \mathrm{KE}_{\mathrm{LEO}}/m \approx 30\,\mathrm{MJ/kg}$ (Eq. 2-2a).

Considering liquid hydrogen (LH_2) as a fuel, instead, we note that while this has a very good specific energy (MJ/kg), it has a rather low energy density ($\mathrm{MJ/m^3}$), with attendant supersonic-drag penalties. Endothermic cooling with LH_2 would rely on the sensible enthalpy of two phase changes (slush to liquid to vapor) and its heat capacity. As with JP8, $Ma_{\min} \approx 4-5$, for similar reasons. The faster chemical kinetics of the H_2-air system, however, coupled with the higher cooling potential of LH_2 would allow a higher upper Mach number, possibly as high as $Ma_{\max} \approx 15$. This yields a better kinetic-energy increment fraction, *i.e.*,

$$\left(\frac{\Delta \mathrm{KE}}{\Delta \mathrm{KE}_{\mathrm{LEO}}}\right)_{4 \leq Ma \leq 15} \approx 41\% \ . \tag{5-8}$$

This, however, still comprises a relatively-small fraction, for a small- payload/-launcher system, considering the cost of the research & development and

complexity (at this time) that the realization of the benefits of an airbreathing stage would require.

We conclude that while scramjets may have an important role to play as hypersonic-propulsion devices,

- the still-awaited research & development required to address the as-yet-unresolved associated science and technology issues, and
- the low kinetic-energy potential (relative to LEO speeds),

preclude them from being considered as the indicated technology for low-cost/small-payload LEO-launcher applications at this time. Their clear potential, however, indicates the need for a continuing effort to resolve the issues and develop the technology so that this potential can be realized.

5.2 A Small, Airlaunched Rocket

The preceding discussion of payload insertion to LEO and the comparative statistics of existing launchers suggest that it should be possible to build an expendable 2-, or 3-stage, airlaunched rocket with a payload mass ratio in the range of (*cf.* Eq. 4-4),

$$1.0\% \lesssim MR \equiv \frac{m_{\rm p}}{m_0} \lesssim 1.5\% \ . \qquad \text{(5-9a)}$$

For a $m_{\rm p} \simeq 50\,{\rm kg}$ (110 lbm) payload, this implies a launch mass in the range of,

$$3600\,{\rm kg} \lesssim m_0 \lesssim 5000\,{\rm kg} \ , \qquad \text{(5-9b)}$$

or,

$$7900\,{\rm lbm} \lesssim m_0 \lesssim 11000\,{\rm lbm} \ . \qquad \text{(5-9c)}$$

Such a launch option combines the high-efficiency of a turbojet-propelled aircraft, for the low-Mach portion of the ascent (*cf.* Figures 9, 10), the higher

I_{sp} for a rocket exhausting at altitude (*cf.* footnote of Section 3), with the proven technology of staged rocket propulsion.

In the interest of low cost, conventional propellants would be used, with a possible kerosene/liquid-oxygen,[17] or liquid-methane/liquid-oxygen,[18] first stage and SRM upper stages (to simplify staging), or an all-SRM-propelled vehicle. If a liquid-propellant stage is indicated, the smaller size could potentially permit expensive fuel/oxidizer pumps to be replaced by a simpler, suitably-pressurized tankage system.

For a low specific launch cost, the lower cost of the vehicle would require some innovation in such subsystems as guidance, which must be amortized over the smaller total cost. They could be built based on relatively-inexpensive, short-integration-time accelerometers, periodically corrected with GPS updates, for example.

The small initial mass (ca. $< 10\,$klbm) would permit launch at an even higher altitude and speed than the *Pegasus*, mitigating the otherwise higher-initial-drag penalty that a smaller vehicle would sustain. Whether such an improved airlaunch option should be considered would depend on available aircraft capabilities and operating costs.

There are no fundamental reasons that specific payload costs should exceed $1250 - 2500\,\$/\text{lbm}$ ($2500 - 5000\,\$/\text{kg}$), for a contract to deliver a large-enough number of launch vehicles. Airlaunch costs could be kept low by exploiting the relatively less onerous air-vehicle modifications that would be required, relative to what was undertaken for the much heavier *Pegasus* vehicle, for example, and might be in the range of $20,000 to $50,000 per single-vehicle launch. Combining these, total launch costs, defined here as marginal costs (air-launch vehicle use, expendable vehicle, fuel, *etc.*, excluding development costs) for a 50 kg payload could be in the range of $150,000

[17] As in the *K-1*.

[18] "To save money, IHI will modify a Russian motor for the J-1's first stage, and Nissan will complete a liquid-methane-fuelled motor that it has in the works for the second stage. Apart from burning more smoothly, and inflicting lower stresses on delicate satellites, liquid methane costs only 1% as much as liquid hydrogen." Economist (8 August 1998) article on Japanese space program.

to $300,000. These represent no more than guestimates of incremental costs, however, predicated on a significant production run and launch schedule of such vehicles. Detailed engineering and cost analysis would be required to substantiate these numbers and provide more-reliable and sharper estimates.

6 SUMMARY AND CONCLUSION

We summarize our findings and conclusions on launch options, at this time, for small payload ($100\,\text{lbm} \lesssim m_\text{p} \lesssim 100\,\text{kg}$) injection to low earth orbit (LEO).

A launch option was considered that entails a rocket-boosted, airbreathing stage. Such a stage holds the greatest promise of increasing payload mass ratio (payload mass to total take-off mass), but relies on science and technology with many unresolved issues, at this time. In view of this promise, the nation might well consider pursuing such potential with a properly-constituted R&D program.

The option that appears to offer the best, low-cost alternative, at this time, is an airlaunched, 2-/3-stage, chemical rocket. At an expected payload mass ratio in the range of $1\% - 1.5\%$, total launch mass would be in the range of $6.5 - 10\,\text{klbm}$, for a 100 lbm payload. Such a launch mass can certainly be accommodated on conventional, subsonic aircraft (B-52, L-1011,), and, possibly on smaller modified, fighter/fighter-bomber, or other aircraft,[19] that would permit a high-altitude launch, at a higher initial Mach number, mitigating aerodynamic-drag considerations. This would provide further gains on the initial kinetic/potential energy imparted to the launcher.

Without conducting a detailed cost analysis, which would anyway depend on specific launches/year scenarios, reliable launch-cost figures are not possible. Nevertheless, assuming a sufficient number of launches per year, it seems to us that total launch costs of $300,000, or less, might be feasible, for a 100 lbm payload.

[19]Removing guns, ammunition, radar, *etc.*, and using only a partially-fueled aircraft to maximize load-carrying capacity and minimize take-off weight.

References

[1] 1998 Aerospace Source Book, *Aviation Week & Space Technology* (12 January 1998), 128–135.

[2] 1999 AEROSPACE SOURCE BOOK, *Aviation Week & Space Technology* (11 January 1999), 135–141.

[3] Braukus, M., Henry K., Williams, K., Castrogioanni, A. & Keel, L. 1998 First Hypersonic Propulsion Hardware Deivered, NASA News (27 August 1998), Release 98–154.

[4] Fortescue, P. & Stark, J., 1995 *Spacecraft Systems Engineering* (2nd edition, John Wiley & Sons, Chistester, England).

[5] Heisler, W. H., Pratt, D. T., Dailey D. D. & Mehtta, U. B. 1994 *Hypersonic Propulsion* (AIAA Education Series, Ed. J. S. Przemienski, AiAA, Washington, DC).

[6] Hill, P. & Peterson, C. 1992 *Mechanics and Thermodynamics of Propulsion* (Addision-Wesley, Reading, MA).

[7] Larson, W. J. & Wertz, J. R. (eds.) 1992 *Space Mission Analysis and Design* (2nd edition, Microcosm, Inc., Torrance, CA, and Kluwer AP, Dordrecht, Netherlands).

[8] Sutton, G. P. & Ross, D. M. 1976 *Rocket Propulsion Elements* (4th edition, John WIley, NY).

Addendum

Note added in proof (August 1999); In discussion above, we did not evaluate fixed-launch options, i.e., launchers that can only service a particular orbit, such as EM rail guns and light-gas guns. In addition to the operational constraints imposed by difficult siting requirements, high development/capital costs, and the restrictions on the range of orbits that can be achieved, thee lofting devices also place added payload-limitations owing to the high-g forces that must be sustained at launch. It is also not clear that they offer reduced specific payload costs, when properly accounted for. This topic is discussed in the upcoming JASON Report (1999) on Space Infrastructure.

DISTRIBUTION LIST

Director of Space and SDI Programs
SAF/AQSC
1060 Air Force Pentagon
Washington, DC 20330-1060

CMDR & Program Executive Officer
U S Army/CSSD-ZA
Strategic Defense Command
PO Box 15280
Arlington, VA 22215-0150

Superintendent
Code 1424
Attn Documents Librarian
Naval Postgraduate School
Monterey, CA93943

DTIC [2]
8725 John Jay Kingman Road
Suite 0944
Fort Belvoir,VA 22060-6218

Dr. A. Michael Andrews
Director of Technology
SARD-TT
Room 3E480
Research Development Acquisition
103 Army Pentagon
Washington, DC 20301-0103

Dr. Albert Brandenstein
Chief Scientist
Office of Nat'l Drug Control Policy
Executive Office of the President
Washington, DC 20500

Dr. H. Lee Buchanan, I I I
Assistant Secretary of the Navy
(Research, Development & Acquisition)
3701 North Fairfax Drive
1000 Navy Pentagon
Washington, DC 20350-1000

Dr. Collier
Chief Scientist
U S Army Strategic Defense Command
PO Box 15280
Arlington, VA 22215-0280

D A R P A Library
3701 North Fairfax Drive
Arlington, VA 22209-2308

Dr. Victor Demarines, Jr.
President and Chief Exec Officer
The MITRE Corporation
A210
202 Burlington Road
Bedford,MA01730-1420

Mr. Frank Fernandez
Director
DARPA/DIRO
3701 North Fairfax Drive
Arlington, VA 22203-1714

Mr. Dan Flynn [5]
Deputy Chief
OSWR
CDT/OWTP
4P07, NHB
Washington, DC 20505

Dr. Paris Genalis
Deputy Director
OUSD(A&T)/S&TS/NW
The Pentagon, Room 3D1048
Washington, DC 20301

Dr. Lawrence K. Gershwin
NIO/S&T
2E42, OHB
Washington, DC 20505

General Thomas F. Gioconda [5]
Assistant Secretary for Defense
US Department of Energy
DP-1, Room 4A019
Mailstop 4A-028
1000 Independence Ave, SW
Washington, DC 20585

Mr. David Havlik
Manager
Weapons Program Coordination Office
MS 9006
Sandia National Laboratories
PO Box 969
Livermore, CA94551-0969

DISTRIBUTION LIST

Dr. Helmut Hellwig
Deputy Asst Secretary
(Science, Technology and Engineering)
SAF/AQR
1060 Air Force Pentagon
Washington, DC 20330-1060

Dr. Robert G. Henderson
Director
JASON Program Office
The MITRE Corporation
1820 Dolley Madison Blvd
Mailstop W553
McLean, VA 22102

J A S O N Library [5]
The MITRE Corporation
Mail Stop W002
1820 Dolley Madison Blvd
McLean, VA 22102

Mr. O' Dean P. Judd
Los Alamos National Laboratory
Mailstop F650
Los Alamos, NM 87545

Dr. Bobby R. Junker
Office of Naval Research
Code 111
800 North Quincy Street
Arlington, VA 22217

Dr. Martha Krebs
Director
Energy Research, ER-1, Rm 7B-058
1000 Independence Ave, SW
Washington, DC 20858

Lt Gen, Howard W. Leaf, (Retired)
Director, Test and Evaluation
HQ USAF/TE
1650 Air Force Pentagon
Washington, DC 20330-1650

Dr. Arthur Manfredi
ZETA Associates
10300 Eaton Drive
Suite 500
FairfaxVA 22030-2239

Dr. George Mayer
Scientific Director
Army Research Office
4015 Wilson Blvd
Tower 3, Suite 216
Arlington, VA 22203-2529

Ms. M. Jill Mc Master
Editor
Journal of Intelligence Community Research
and Development (JICRD)
Investment Program Office (IPO)
1041 Electric Avenue
Vienna,VA 20180

Dr. Thomas Meyer
DARPA/DIRO
3701 N. Fairfax Drive
Arlington, VA 22203

Dr. Bill Murphy
ORD
Washington, DC 20505

Dr. Julian C. Nall
Institute for Defense Analyses
1801 North Beauregard Street
Alexandria, VA 22311

Dr. Ari Patrinos [5]
Associate Director
Biological and Environmental Research SC-7
US Department of Energy
19901 Germantown Road
Germantown,MD 207874-1290

Dr. Bruce Pierce
USD(A)D S
The Pentagon, Room 3D136
Washington, DC 20301-3090

Mr. John Rausch [2]
Division Head 06 Department
NAVOPINTCEN
4301 Suitland Road
Washington, DC 20390

DISTRIBUTION LIST

Records Resource
The MITRE Corporation
Mailstop W115
1820 Dolley Madison Blvd
McLean, VA 22102

Dr. Fred E. Saalfeld
Director
Office of Naval Research
800 North Quincy Street
Arlington, VA 22217-5000

Dr. Dan Schuresko
O/DDS&T
OSA/ATG
Room 23F20N, WF-2
Washington, DC 20505

Dr. John Schuster
Submarine Warfare Division
Submarine, Security & Tech
Head (N875)
2000 Navy Pentagon Room 4D534
Washington, DC 20350-2000

Dr. Michael A. Stroscio
US Army Research Office
P. O. Box 12211
Research Triangle Park, NC27709-2211

Ambassador James Sweeney
Chief Science Advisor
USACDA
320 21st Street NW
Washington, DC 20451

Dr. George W. Ullrich [3]
Deputy Director
Defense Special Weapons Agency
6801 Telegraph Road
Alexandria, VA 22310

Dr. David Whelan
Director
DARPA/TTO
3701 North Fairfax Drive
Arlington, VA 22203-1714

Dr. Edward C. Whitman
US Naval Observatory
Nval Oceanographers Office
3450 Massachusetts Ave, NW
Washington, DC 20392-5421